ACS Energy LETTERS

Editors' Choice

http://pubs.acs.org/journal/aelccp

The Potential of Zero Total Charge Predicts Cation Effects for the Oxygen Reduction Reaction

Jay T. Bender, Rohan Yuri Sanspeur, Angel E. Valles, Alyssa K. Uvodich, Delia J. Milliron, John R. Kitchin, and Joaquin Resasco*

Cite This: *ACS Energy Lett.* 2024, 9, 4724–4733

Read Online

ACCESS | Metrics & More | Article Recommendations | Supporting Information

ABSTRACT: **Cation effects are frequently observed for electrochemical reactions that take place at strongly reducing potentials. But a clear understanding of when cation effects will be observed for chemistries like the oxygen reduction reaction (ORR), which occurs at more mildly reducing potentials, has not been developed. Here, based on the results of experimental and computational studies, we propose that the potential of zero total charge (PZTC) predicts whether ORR rates will be influenced by alkali metal cation size. For metals whose PZTC is positive of the ORR potential window (Pt, Ir, Ru, and Au), the surface is negatively charged during catalysis, allowing cations to accumulate in the double layer and influence the stability of reaction intermediates. For these metals, ORR rates increase with cation size ($Li^+ < Na^+ < K^+ < Cs^+$). We argue that interfacial cations decrease *OH poisoning over strongly binding catalysts whose rates are limited by product desorption and decrease the apparent activation barrier for O_2 adsorption over weakly binding catalysts. Conversely, for metals whose PZTC is negative of the ORR potential window (Ag and Pd), the surface is positively charged; therefore, cations are electrostatically repelled from the surface under reaction conditions. Their corresponding ORR rates are insensitive to the electrolyte composition.**

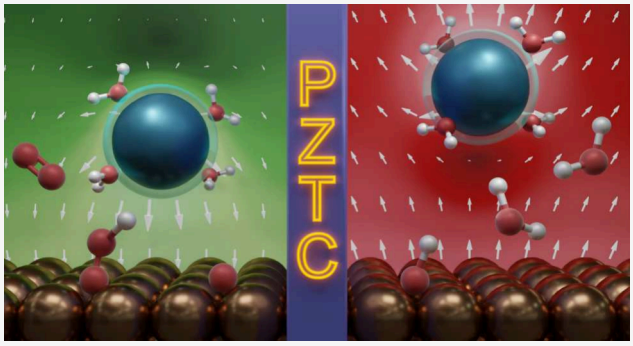

Technologies based on electrocatalysis hold promise for decarbonizing chemical manufacturing processes and storing energy from intermittent renewable electricity sources in chemical bonds.[1] Extensive research has been done to advance these technologies by developing highly active and stable electrocatalyst materials.[2,3] Complementary to these efforts, there has also been significant recent interest in enhancing catalytic performance by tuning the composition of the electrolyte in which the reaction takes place.[4] Specifically, the identity of alkali metal cations in the electrolyte has been shown to consistently affect rates for a variety of electrocatalytic reactions including CO_2 reduction, hydrogen evolution, hydrogen oxidation, and methanol oxidation.[5−7] However, for electrochemical reactions occurring at more positive electrochemical potentials, such as the oxygen reduction reaction (ORR) and the oxygen evolution reaction, cation effects are less general.[8−10] For instance, for the ORR in alkaline electrolytes, cation effects are only sometimes observed, depending on the nature of the catalyst surface.[7,11−15] An explanation for why cation effects are observed for some catalytic materials, but not for others, is needed.

Here, we argue that the metal's potential of zero total charge (PZTC), or the potential at which the surface carries no excess charge in the presence of adsorbates, effectively predicts whether cation effects will be observed over a particular metal surface. We use the ORR as a probe reaction because its equilibrium potential lies close to the potential of zero charge (PZC) of many transition metals. Additionally, the ORR is practically important for fuel cell and water purification technologies.[16−19] Experimentally, we measured ORR rates and selectivities over a series of polycrystalline and carbon-supported metal catalysts (Pt, Ir, Ru, Au, Ag, and Pd) in LiOH, NaOH, KOH, and CsOH electrolytes. Over Pt, Ir, Ru and Au, ORR rates increased with cation size ($Li^+ < Na^+ < K^+ < Cs^+$)

Received: July 12, 2024
Revised: August 11, 2024
Accepted: August 29, 2024

https://doi.org/10.1021/acsenergylett.4c01897
ACS Energy Lett. 2024, 9, 4724−4733

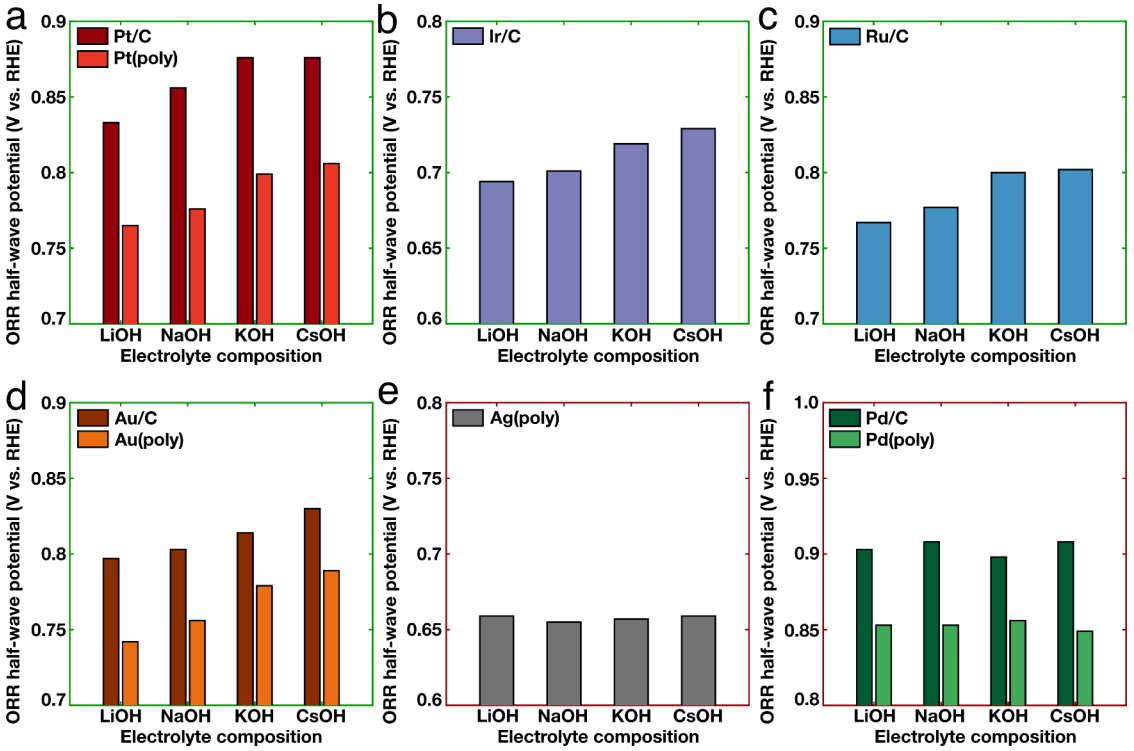

Figure 1. Cation effects for the ORR over transition metal surfaces. Over (a) Pt/C and Pt(poly), (b) Ir/C, (c) Ru/C, and (d) Au/C and Au(poly), increasing cation size increases ORR activity quantified by the half-wave potential (V vs RHE). Over (e) Ag(poly) and (f) Pd/C and Pd(poly) ORR rates are not affected by cation size. All electrolytes contained 0.1 M XOH (X = Li, Na, K, Cs). The half-wave potentials were extracted from cyclic voltammetry scans in the anodic direction and are corrected for 85% of the solution resistance.

while rates were insensitive to cation identity over Ag and Pd. ORR selectivity was not affected by cation size over Pt, Ir, Ru, Ag, and Pd but increased to favor H_2O_2 production with increasing cation size over Au.

To explain this behavior, we propose that the potential window where the ORR occurs for a particular metal relative to its PZTC predicts whether cation effects will be observed for the ORR. For metals where the ORR occurs negative of the PZTC, the negative charge of the surface during catalysis drives cations toward the interface where they modify the electric field experienced by the ORR reaction intermediates. Over metals where the ORR occurs positive of their PZTC, the surface is positively charged during catalysis, so it repels cations from the interface. Thus, the electric field experienced by ORR reaction intermediates at the interface is the same regardless of cation size. Surface charge density has been used to understand trends with cation size for the hydrogen evolution reaction and the electrochemical CO_2 reduction reaction, but has not been used to understand cation effects on the ORR or to predict when cation effects will be observed.[20−22]

The central role of the PZTC in governing cation effects is supported by our density functional theory (DFT) calculations, which estimate the PZTC of low Miller index metal surfaces, accounting for the presence of relevant coverages of adsorbed hydroxide (*OH) and adsorbed oxygen (*O). Our study rationalizes why cation effects are observed for the ORR over some metals and not others and ultimately furthers two key criteria for electrochemical reactions to be sensitive to the choice of electrolyte cation: the reaction needs to occur at a potential negative of the metal's PZTC and the rate-determining elementary steps need to involve intermediates or transition states that are field-sensitive. These criteria may provide insights for predicting cation effects for novel electrochemical reactions and identify future opportunities to optimize electrocatalytic rates by changing the environment surrounding the active site.

UNDERSTANDING HOW CATIONS AFFECT THE ORR MECHANISM

To examine the effect of alkali metal cations on the ORR, rotating ring-disk electrode (RRDE) activity measurements were conducted over a series of commercially available polycrystalline metals (Pt(poly), Au(poly), Ag(poly), Pd(poly)) and carbon-supported metal nanoparticle catalysts (Pt/C, Ir/C, Ru/C, Au/C, Pd/C). Cyclic voltammograms were measured in an Ar-saturated electrolyte of pH = 13 containing 0.1 M XOH (where X = Li, Na, K, Cs) (Figure S1) followed by the same electrolyte saturated with O_2. To report ORR activity, the current response of the Ar-saturated solutions was subtracted from the current response of the O_2-saturated solutions (Figure S2).[23] To investigate if observed trends in total ORR current with cation size were due to changes in ORR selectivity between the $4e^-$ and $2e^-$ pathways, the Pt ring was held at 1.1 V versus RHE and the ring current was recorded at each disk potential (Figure S3). Selectivity for the $2e^-$ ORR was calculated by dividing the ring current by the disk current and scaling the quotient by the ring collection efficiency (Figure S4).[24] The ring collection efficiency in each electrolyte was determined using $K_3Fe(CN)_6$ (Figure S5).[24] The RRDE selectivity trends were confirmed using Koutecký−Levich analysis, by measuring ORR activity at 100, 400, 900, 1600, and 2500 rpm (Figures S6−S14). Finally, to understand why ORR rates depend on cation size, we measured the hydroxide reaction order over the Pt(poly)

https://doi.org/10.1021/acsenergylett.4c01897
ACS Energy Lett. 2024, 9, 4724−4733

catalyst in 0.1, 0.2, 0.5, and 1.0 M XOH electrolytes and apparent activation barriers over the Au(poly) catalyst in each 0.1 M electrolyte between 25 and 50 °C (Figures S15–S18). Further experimental details are available in the Supporting Information (SI) (Sections S1–S5).

Figure 1 shows two different trends among transition metal catalysts. Over Pt/C, Pt(poly), Ir/C, Ru/C, Au/C, and Au(poly), ORR rates increase with alkali metal cation size. Here, increases in activity are represented by an increase in the half-wave potential (Figure 1a–d) versus the reversible hydrogen electrode (RHE). The half-wave potential is the electrode potential required to reach a current density that is halfway between zero and the mass-transfer-limited current value. Conversely, ORR rates over Ag(poly), Pd/C, and Pd(poly) are not affected by cation size (Figure 1e,f). ORR rates over carbon-supported metal nanoparticle catalysts were greater than rates over polycrystalline metal catalysts due to their higher surface area (Figure 1a,d,f). Our results are consistent with prior work showing increasing ORR activity with cation size over Pt/C,[7,11,25,26] Pt(poly),[7,27] Ir,[13] and Ru[13] and no cation effect over Ag[28,29] and Pd.[11,15] Finally, all measured ORR activity from this study shows good agreement with benchmark data in prior work.[7,11,25−30] Benchmark comparisons are available in the SI (Section S9 and Figure S19).

For the ORR, H_2O_2 desorbs as a product if the O−O bond in *OOH is not broken (eq 1b). Gold exhibits relatively high selectivity to H_2O_2 due to its exceptionally weak interaction with oxygen. All materials except Au(poly) and Au/C showed full selectivity for the 4e$^-$ ORR pathway toward H_2O (Figure S4), consistent with prior work,[26,28,31,32] while selectivity for the 2e$^-$ ORR pathway toward H_2O_2 increased with cation size over Au(poly) and Au/C (Figure 2).[31,32] Koutecký−Levich

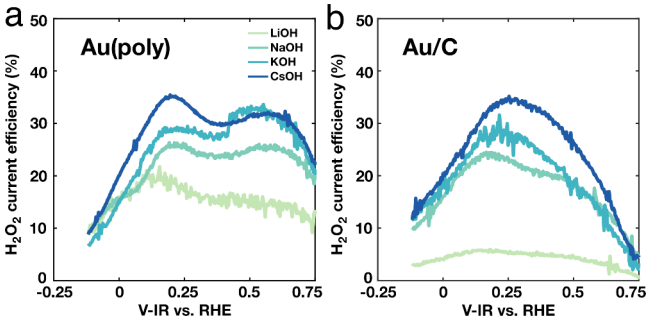

Figure 2. Cation effects on selectivity for the 2e$^-$ ORR pathway toward H_2O_2 over Au. RRDE measurements indicated increasing selectivity toward H_2O_2 with cation size over (a) Au(poly) and (b) Au/C. All electrolytes contained 0.1 M XOH (X = Li, Na, K, Cs). The ring was held at 1.1 V vs RHE, and the current response was measured during simultaneous cyclic voltammetry at 10 mV/s and 1600 rpm at the disk. The data shown represent the scan in the anodic direction and are corrected for 85% of the solution resistance.

analysis confirmed the RRDE selectivity trends (Figures S6–S14). Finally, the same trends in Figure 1 and Figure S2 were observed when accounting for only the 4e$^-$ ORR current.

To understand the effect that cations have on the ORR rates, we can consider the ORR mechanism. Here, we assume the ORR proceeds through an associative mechanism via 4 proton-coupled electron transfer (PCET) elementary steps:[33−35]

$$O_2 + (H^+ + e^-) + (*) \rightleftharpoons {}^*OOH \quad (1a)$$

$${}^*OOH + (*) \rightleftharpoons {}^*O + {}^*OH \quad (1b)$$

$${}^*O + (H^+ + e^-) \rightleftharpoons {}^*OH \quad (1c)$$

$$2({}^*OH + (H^+ + e^-) \rightleftharpoons H_2O + (*)) \quad (1d)$$

where (*) denotes a catalytic active site. We note that although the mechanism is written as a series of PCET steps, the H^+ source under alkaline conditions is water via its dissociation ($H_2O \rightarrow H^+ + OH^-$), rather than protons/hydronium ions. It is generally accepted that the entry step of the reaction (eq 1a) is rate limiting over noble metals such as Au and Ag while the removal of adsorbed hydroxide (eq 1d) is rate limiting over reactive metals such as Pt, Ir, Ru, and Pd.[17,34] Tafel analysis of the kinetic current density showed an increase in Tafel slope from ∼60 to ∼120 mV/dec with increasing overpotential over all metal surfaces in all electrolyte compositions (Figure S20). Recent work has argued that this shift in Tafel slope is due to changes in *OH surface coverage (θ_{OH}) and does not necessarily mean that all metals share the same rate limiting step.[35] More details on the Tafel analysis and kinetic modeling are given in the SI (Section S10, Figures S21 and S22).

Previous studies have attributed cation effects to changes in interfacial electric fields and the resulting impact on adsorbed reaction intermediates.[5,36−41] Strong interfacial fields (de)-stabilize intermediates and transition states with large dipole moments and polarizabilities,[5,36,41] and field strength increases with alkali metal cation size.[5,20] The resulting influence on rates depends on the field sensitivity of the adsorbates involved in kinetically relevant elementary steps, the orientation of their dipole, and the surface charge. For example, for electrochemical CO_2 reduction, the effect of the field is most notable on CO_2 activation and C−C bond formation steps.[36,39] Applying this model here, the relevant reaction intermediates of the oxygen reduction reaction (*OOH, *O, and *OH) have large dipole moments, meaning that changes in interfacial field strength could have a strong influence on ORR rates.[42,43] In particular, recent DFT calculations suggest that an increasingly negative electric field toward the catalyst surface could facilitate O_2 activation on weakly binding catalysts and slightly destabilize adsorbed hydroxide on strongly binding catalysts.[42]

Alternatively, other work has implicated noncovalent interactions between electrolyte cations and adsorbed hydroxide to explain observed cation effects.[7] The size effect stems from an increase in the concentration of hydrated cation clusters with increasing cation hydration energy and decreasing size.[7] These clusters "block" metal active sites, with the extent of site-blocking being dependent on the oxophilicity of the metal.[13] These models suggest that a high θ_{OH} is necessary to observe cation effects. Consistent with that requirement, these authors did not observe cation effects for the ORR over Au catalysts.[12,44] Similarly, in this study, we did not observe a cation effect over Ag(poly) (Figure 1e). However, in this study, we observe a notable cation effect over both Au/C and Au(poly) (Figure 1d). A model based on cations coordinating with *OH to form site-blocking complexes would fail to explain why cation effects were observed over Au but not over Ag and the fact that cation effects are observed for other reactions where *OH does not play a significant role.[5,20,45−47]

Knowing the elementary steps that control rates over different catalysts, we can experimentally interrogate the role

https://doi.org/10.1021/acsenergylett.4c01897
ACS Energy Lett. 2024, 9, 4724−4733

of cation size for each class of transition metal. To understand cation effects for strongly binding catalysts whose ORR rates are limited by *OH removal (eq 1d), OH^- concentration dependent measurements were conducted over Pt(poly) (Figure S15). The reaction order in XOH (where X = Li, Na, K, or Cs) (δ_{XOH}) becomes less negative with applied potential and increasing cation size (Figure 3a). The negative

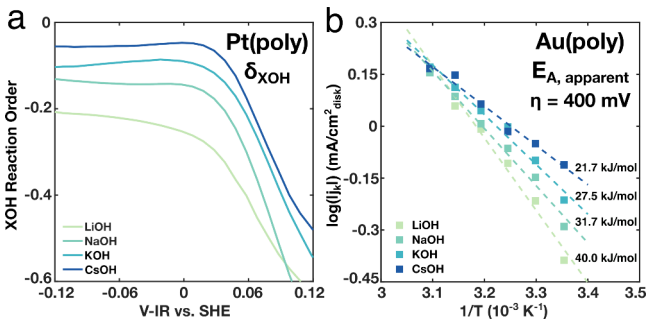

Figure 3. Understanding the role of cation size over strongly binding and weakly binding ORR catalysts. (a) The reaction order in hydroxide (δ_{XOH}) increases with cation size over Pt(poly). These measurements were conducted in 0.1, 0.2, 0.5, and 1.0 M electrolyte concentrations. (b) Arrhenius plot used to extract apparent activation energies from kinetic current density (j_k) at a fixed overpotential of η = 400 mV for ORR over Au(poly). $E_{A,apparent}$ decreases with cation size over Au(poly).

order indicates that *OH poisons strongly binding catalysts, including Pt. δ_{XOH} increasing with cation size provides evidence for the idea that the extent of *OH poisoning decreases with increasing cation size.[7,13] We determined δ_{XOH} on the standard hydrogen electrode (SHE) potential scale because we were interested in determining how cation-mediated electric fields influence *OH desorption, and the electric field strength depends on the absolute potential of the electrode. We further compared ORR rates in electrolytes containing 0.1 M NaOH + 0.1 M $NaClO_4$ (Figure S16a) and 0.1 M KOH + 0.1 M $KClO_4$ (Figure S16b) with ORR rates in electrolytes containing only 0.1 M NaOH or KOH to examine the role of X^+ concentration separately from OH^- concentration. We observed that X^+ concentrations of >0.1 M did not affect kinetic ORR rates. Further analysis was precluded by the fact that some alkali metal salts are insoluble at high concentrations or contain anions that are known to strongly adsorb to metal catalysts and influence reactivity.[48] To understand the influence of cations on the ORR over weakly binding catalysts whose rates are limited by O_2 adsorption (eq 1a), we conducted temperature-dependent activity measurements over Au(poly) (Figure S17). Figure 3b shows Arrhenius plots for the ORR in each electrolyte. At a fixed overpotential of η = 400 mV, we observed that the apparent activation barrier ($E_{A,apparent}$) decreased from 40.0 to 21.7 kJ/mol with increasing cation size. We also determined $E_{A,apparent}$ over a fixed applied potential range and similarly found that $E_{A,apparent}$ decreased with increasing cation size (Figure S18). Both experimental sets of data in Figure 3 are consistent with recent DFT calculations which demonstrate that increasingly negative interfacial fields increase ORR rates over both strongly binding and weakly binding catalysts.[42] The reaction order results (Figure 3a) are compatible with arguments based on cations forming site-blocking complexes with *OH, but the $E_{A,apparent}$ trends (Figure 3b) are not. The measurements in Figure 3b and Figure S18 suggest that cations' primary role is not to block active sites. A change in the number of accessible or highly active sites would change only the intercept of each Arrhenius plot and not its slope.

UNDERSTANDING WHEN CATION EFFECTS WILL BE OBSERVED FOR THE ORR

Having identified that cations can modulate reaction rates, likely through a field effect, we now attempt to rationalize why cation effects were observed for the ORR over some metal catalysts but not for others. The concentration of hydrated cations at the solid−liquid interface increases as the electrode is polarized to increasingly negative potentials relative to the surface's potential of zero charge. This can be described using the surface charge density (σ), according to[21]

$$\sigma = C_{gap} \cdot (E_{SHE} - E_{PZC}) \quad (2)$$

where C_{gap} is the gap capacitance,[20,49] E_{SHE} is the applied potential versus the standard hydrogen electrode, and E_{PZC} is the potential of zero charge. σ is roughly proportional to the interfacial electric field. A higher interfacial cation concentration correlates with an increased surface charge density and larger interfacial electric field strength.[20] When $E_{SHE} < E_{PZC}$ and σ is negative, cations accumulate at the electrochemical interface. At a fixed potential E_{SHE}, the interfacial cation concentration changes due to differences in the cation solvation energy. Smaller, more strongly solvated cations are less willing to break their interactions with solvent molecules and interact with the electrode.[20,42] Thus, with increasing cation size, the interfacial cation concentration and C_{gap} increases, leading to larger σ and a stronger interfacial field. When $E_{SHE} > E_{PZC}$, and σ is positive, cations do not accumulate at the interface, resulting in insignificant differences in the field experienced by adsorbates and thus no cation effects.[50]

Reactions in which cation effects are consistently observed, such as the alkaline hydrogen evolution reaction and electrochemical CO_2 reduction, occur at potentials significantly negative of the PZC of transition metals. On the other hand, the ORR occurs at more positive potentials, closer to the PZC of metals.[51−54] We propose that the PZTC can serve as a descriptor to predict whether cation effects will be observed for the ORR. We use the PZTC, rather than the PZC, as it accounts for adsorbate coverage, which can be high for some metals during the ORR. However, we compare our experimental results and ensuing PZTC calculations with literature PZC values because literature PZTC values specific to the alkaline oxygen reduction reaction are not available. We note that reliably measuring the PZC in the absence of electrolyte adsorption, known as the potential of zero free charge (PZFC), is challenging and that reported literature PZC values may be more representative of the metal's PZTC.[55] For further discussion of the differences between the PZC, PZTC, and PZFC, we refer readers to prior work.[53,56,57] For metals that we experimentally observed to display cation effects for the ORR (Figure 1a−d), their experimental ORR potential window was negative of previously published PZC values for close-packed metal surfaces, with the exception of Ru. (Table 1).[51,52] The resulting negative surface charge would electrostatically attract cations to the catalyst interface, where they can influence ORR rates (Figure 4a). For Ru, we attribute the discrepant prediction to high *O coverage, which is captured by our PZTC calculations, as discussed below. For metals that

https://doi.org/10.1021/acsenergylett.4c01897
ACS Energy Lett. 2024, 9, 4724−4733

Table 1. Comparison between Experimental Half-Wave Potentials, Available Literature PZC Values, and PZTC Values of Pt, Ir, Au, Ag, Pd (111), and Ru (0001) Surfaces[a]

Catalyst	Half-wave V (vs SHE)	Literature PZC (vs SHE)	Our PZTC (vs SHE)
Pt/C	0.11; Cation effect	0.27;[51] 0.2;[52] Predicts cation effect	0.92; Predicts cation effect
Pt(poly)	0.032; Cation effect	0.27;[51] 0.2;[52] Predicts cation effect	0.92; Predicts cation effect
Ir/C	−0.048; Cation effect	−0.02;[51] 0.13;[51] Predicts cation effect	0.68; Predicts cation effect
Ru/C	0.033; Cation effect	−0.48;[64] Predicts no cation effect	0.30; Predicts cation effect
Au(poly)	0.012; Cation effect	0.51;[51] 0.50;[52] Predicts cation effect	0.33; Predicts cation effect
Ag(poly)	−0.11; No cation effect	−0.45;[51] −0.70;[51] −0.60;[52] Predicts no cation effect	−0.39; Predicts no cation effect
Pd(poly)	0.089; No cation effect	0.21;[54] Predicts cation effect	0.58; Predicts cation effect

[a]In each table entry we note if cation effects were experimentally observed and if PZC/PZTC values would predict cation effects.

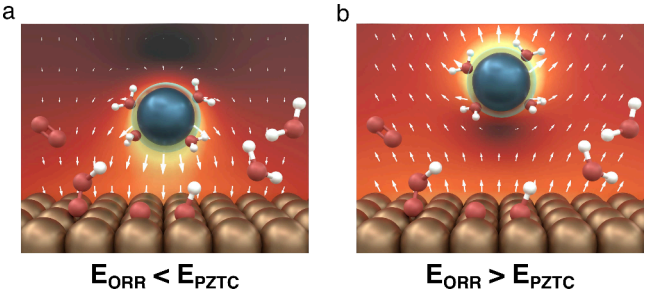

Figure 4. Proposed scheme for the PZTC predicting cation effects for the oxygen reduction reaction. (a) Over metal surfaces where the ORR occurs negative of the PZTC, the negative surface charge density ($-\sigma$) allows cations to accumulate near the surface to mediate the electric field experienced by ORR reaction intermediates. (b) Over metal surfaces where the ORR occurs positive of the PZTC, the positive surface charge density ($+\sigma$) prevents cations from accumulating at the surface, resulting in a low cation concentration and no cation effect.

did not show cation effects (Figure 1e,f), their experimental ORR potential window was positive of previously published PZC values (Table 1), resulting in a positively charged surface that repels cations from the interface (Figure 4b).[51,52] Consistent with this hypothesis, recent experimental work used *in situ* X-ray photoelectron spectroscopy to confirm the presence of cations at electrocatalytic interfaces negative of their PZC, concurrent with an observation of cation effects for the ORR.[43]

To understand whether these effects could be captured computationally, we performed DFT calculations on the (111), (100), and (110) surfaces of Pt, Ir, Au, Ag, and Pd and on the (0001), (10−10), and (10−11) surfaces of Ru using the semiautonomous *WhereWulff* workflow.[58] As we expected simulating adsorbate coverage would be important to estimating surface charge, we used *WhereWulff* to calculate surface Pourbaix diagrams including *OH and *O adsorbates to determine the relevant ORR coverages under experimental conditions (Figures S23−S28). Then, *WhereWulff* artificially applied an electric field at each ORR elementary step at 0.80 V versus RHE at the coverage predicted by the metal's surface Pourbaix diagram by changing the excess number of electrons in the metal slab. This potential was selected because experimentally all metals displayed a Faradaic ORR current at 0.80 V versus RHE. Next, *WhereWulff* calculated the slab's change in electric potential versus SHE in response to applying the field.[59,60] Finally, the PZTC was determined by fitting these single-point data to a continuous parallel plate capacitor model which contained the PZTC as a variable (Figure 5 and Figures S29−S34).[61] Generally, the adsorbate coverage predicted at the PZTC was the same as the coverage at 0.80 V vs RHE (Figures S23−S28). We note here that the calculated PZTC differs slightly from the PZTC derived from experimental measurements. The calculations allow us to estimate the potential at which the metal surface is free of excess charge, accounting for adsorbate coverage, but does not accurately capture the charge transferred from the adsorbate to the surface experimentally during the chemisorption process. Computational details are available in the SI (Section S6).

Figure 5 shows the free energy of each metal as a function of applied potential with different adsorbates present. The free energy follows the expected quadratic behavior with each adsorbate having a different response to the interfacial field depending on its orientation, dipole moment, and polarizability.[36,42,61] The maxima of each parabola, plotted as a dashed bar along the *x*-axis, correspond to the PZTC at that elementary step based on each of the reaction intermediates. Beneath each plot are illustrations of the metal surfaces at each elementary step with the surface coverage termination returned by *WhereWulff* representative of ORR reaction conditions. Finally, the experimental ORR half-wave potential in 0.1 M KOH is plotted as a dashed blue line to qualitatively compare the experimental results with our model. Over Pt(111), Ir(111), Ru(0001), Au(111), and Pd(111) surfaces, the calculated PZTC was positive of the experimental ORR potential window (Figure 5a−d,f). On the other hand, over Ag(111), the calculated PZTC was negative of the experimental ORR potential window (Figure 5e). Our computational model rationalizes the experimentally observed cation effects over Pt, Ir, Ru, and Au catalysts (Figure 1a−d) and the absence of cation effects over Ag (Figure 1e). All Pd surfaces had calculated PZTC values positive of their ORR potential window (Figure 5f and Figure S34) despite no cation effects being experimentally observed (Figure 1f). Possible reasons for this discrepancy are discussed later on. Otherwise, the same trends for metals with and without cation effects were also observed over all other metal (100), (110), (10−10), and (10−11) surfaces (Figures S29−S33).

Our model accurately predicted that cation effects should be observed over Au/C and Au(poly) (Figure 5d) despite *WhereWulff* returning a bare surface termination over Au(111) and Au(110) (Figure S26a,c). This suggests that high θ_{OH} is not a requirement to observe cation effects, and that cations' primary role in mediating ORR catalysis is not site blocking. Instead, our $E_{A,apparent}$ results (Figure 3b) suggest that increasing cation size lowers the barrier for O_2 adsorption (eq 1a) over Au by modifying the interfacial electric field strength. This is supported by prior microkinetic modeling studies which show that strong negative fields stabilize $*O_2$ or *OOH. As O_2 adsorption (eq 1a) is the sole kinetically relevant step over Au surfaces, this predicted an increase in ORR rates.[42] While *WhereWulff* predicted a 1/8 monolayer *OH termination over Au(100) (Figure S26b), consistent with prior studies,[61] all three Au facets studied had calculated PZTC values positive of the experimental ORR potential window

https://doi.org/10.1021/acsenergylett.4c01897
ACS Energy Lett. 2024, 9, 4724−4733

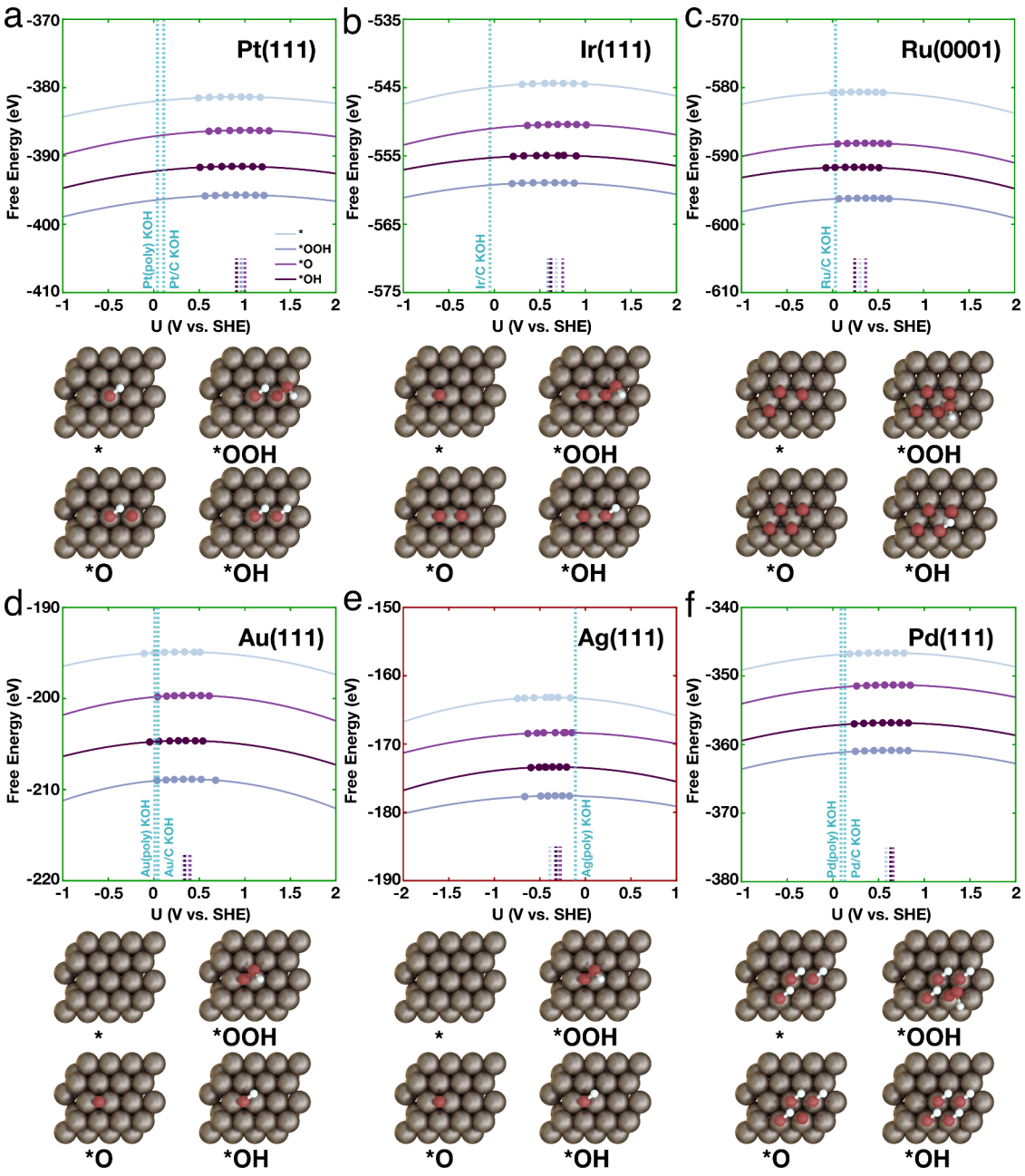

Figure 5. PZTC calculations for metal close-packed surfaces at each ORR elementary step. Over (a) Pt(111), (b) Ir(111), (c) Ru(0001), (d) Au(111), and (f) Pd(111), the PZTC for all ORR intermediates (colored dashed bars) are positive of the experimental ORR half-wave potentials (dashed blue vertical lines). Over (e) Ag(111), the PZTCs for all ORR elementary steps are negative of the ORR half-wave potential. Beneath each plot are illustrations of the metal surfaces with adsorbate coverage representative of ORR experimental conditions that the calculations were performed on.

(Figure 5d and Figure S32). Furthermore, cation effects were not experimentally observed over Pd despite *WhereWulff* returning an *OH terminated surface over all three facets (Figure S28), further suggesting that high θ_{OH} does not generally predict whether cation effects will be observed. The influence of cations on ORR reaction rates is thus more consistent with a field effect than prior models that attribute ORR cations forming site-blocking complexes with adsorbed ORR reaction intermediates.

In our proposed mechanism, the relationship between the PZTC and the experimental potential where the ORR occurs should govern the emergence of cation effects. The half-wave potentials from our experiments in 0.1 M KOH electrolytes are compared to our calculated PZTC values for the close-packed surfaces and to available literature PZC values in Table 1. The same comparisons are available for the (100) and (110) or (10−10) and (10−11) surfaces in the SI (Section S12, Tables S1 and S2). The strongly binding metals (Pt, Ir, Ru, and Pd) have calculated PZTC values significantly more positive than the literature PZC values. This shift likely occurs because these reactive metal surfaces have a high *OH or *O coverage under ORR conditions. Specifically adsorbed oxygen intermediates withdraw electrons from the metal surface, leading to a significant offset between PZC and PZTC values.[61] For the Ru catalyst, accounting for the specific adsorption of *O in the PZTC calculations allowed the model to properly predict

https://doi.org/10.1021/acsenergylett.4c01897
ACS Energy Lett. 2024, 9, 4724−4733

cation effects compared to the PZC value from the literature. Weakly binding metals (Au and Ag) have calculated PZTC values that are closer to the PZC values from the literature because these surfaces are free of significant coverages of adsorbates, which alter the surface charge of the metal. We calculated PZC values of completely bare metal surfaces and compared them to our PZTC values (Tables S3−S5). Other than the Ru catalyst, calculating the PZTC accounting for specific adsorption did not change the prediction of whether cation effects would be observed compared to using our calculated PZC. Finally, we compared our PZC and PZTC values from Tables S3−S5 with available literature metal work function values (Figure S35).[62] The linear relationship between the PZC and work function (Figure S35a) agrees well with prior reports.[63] Including *OH or *O coverage slightly increases the PZC, and this offset between the PZTC and PZC was greater for more oxophilic metals (Pt, Ir, Ru, and Pd) than for noble metals (Au and Ag) (Figure S35b).

Accurately estimating the PZTC of transition metal surfaces with computational methods is challenging.[52,60,65,66] Using implicit solvation models, as we have done in this work, introduces inaccuracies, particularly for metals with work functions exceeding ∼5.5 eV such as Pt, Ir, and Pd. These reactive metals strongly adsorb water, causing a greater electron redistribution and larger difference between the metal's work function and PZC.[67] Continuum solvation models are not able to accurately account for specific adsorption of water, causing an overestimation of the PZC by ∼0.40 V for reactive metals compared to noble metals.[52,62,65] Here, if the calculated PZTC values for Pt and Ir were lowered by 0.40 V, cation effects would still be correctly predicted across all three Pt and Ir surface terminations. For Pd, lowering its calculated PZTC by 0.40 V would result in a PZTC closer to experimental PZC values. Using this PZTC, we would predict cation effects to be observed over Pd(111) but not over Pd(100) and Pd(110). Interestingly, this exact facet dependence is observed in studies over Pd single-crystal surfaces.[15] The absence of cation effects in our polycrystalline Pd data may reflect activity from (100) or (110) terminations or less highly coordinated Pd sites. Overall, our continuum solvent calculations were able to capture nearly all of the observed experimental trends while allowing us to understand the influence of adsorbate coverage.

Explicit solvent calculations have also been considered to calculate the PZC of metal surfaces. Beyond the significant increase in computational cost, use of an explicit solvent may not increase the accuracy of PZC calculations[68] and introduces additional uncertainty due to the difficulty in properly equilibrating the solvent/vacuum and solvent/catalyst interfaces.[69] Even for well studied surfaces such as Pt(111), PZC values calculated using *ab initio* molecular dynamics simulations vary from 0.2 to 0.6 V versus SHE.[52,70−72] Alternatively, correlations between descriptors such as water or *OH binding energies can be used to estimate PZC values to avoid having to do costly *ab initio* molecular dynamics calculations.[64,67] Ideally, experimentally measuring the PZTC for metals under ORR reaction conditions would provide the most accuracy.[56,73−76]

Regardless of the model used to explain cation size effects, the electrochemical conditions need to be favorable to provide a driving force to bring alkali metal cations to the catalyst surface (Figure 4a). To satisfy this electrostatic requirement, the reaction needs to occur negative of the metal's PZTC. We demonstrated this principle by comparing Pt, Ir, Ru, and Au catalysts (Figure 1a−d) whose ORR operating potentials were negative of their calculated PZTC values (Figure 5a−d) with the Ag catalyst (Figure 1e) whose ORR operating potential was positive of its calculated PZTC value (Figure 5e). We hypothesize the reversal of surface charge for Ag would repel cations from the surface and eliminate cation size dependence (Figure 4b).[50] Furthermore, to observe cation effects, the reaction must involve reaction intermediates with significant dipole moments or polarizabilities. We have previously observed the absence of cation effects for other reactions under conditions when the reaction occurs negative of the metal's PZC.[6] However, these mechanisms involve intermediates that do not have significant surface dipole moments.

In this study, we investigated the effects of alkali cation size on the activity of transition metal catalysts for the oxygen reduction reaction in alkaline conditions. ORR reaction rates increased with cation size ($Li^+ < Na^+ < K^+ < Cs^+$) over several polycrystalline (Pt(poly) and Au(poly)) and carbon-supported nanoparticle (Pt/C, Ir/C, Ru/C, and Au/C) catalysts. Over strongly binding catalysts, whose rates are limited by ORR product desorption, ORR rates increased with alkali metal cation size due to decreased *OH poisoning. Over weakly binding catalysts, whose rates are limited by O_2 adsorption, increasing cation size decreased apparent activation barriers. We propose that when the ORR occurs negative of the PZTC, the negatively charged surface allows cations to accumulate in the double layer and influence reaction rates. On the other hand, over polycrystalline and carbon-supported nanoparticle Ag and Pd catalysts, the choice of alkali metal cation had no effect on ORR rates. We attribute this to the ORR occurring positive of these metals' PZTC, preventing cations from accumulating at the catalyst surface. This hypothesis was supported by DFT calculations which estimated the PZTC, accounting for specific adsorption of ORR intermediates to mimic experimental conditions. We hypothesize that trends with cation size depend on the interfacial cation concentration, with larger, weakly solvated cations more readily approaching the electrode surface. Taken together, this study furthers two key criteria for electrocatalytic reaction mechanisms to show cation effects: they must involve reaction intermediates that are field-sensitive and must occur negative of the metal's PZTC in order for cations to be present at the interface.

Developing fundamental principles to rationally influence the performance of electrocatalysts through electrolyte engineering is key to advancing the performance of electrochemical systems. Through this work, we hope to have contributed to this understanding. This work could help identify opportunities in which alkali metal cations can be used to enhance electrocatalytic rates in practical devices. Continued experimental studies that use kinetic or spectroscopic techniques to understand electrochemical reaction mechanisms and the structure of electrochemical interfaces would be of great value.[77−83] Combining these studies with advanced computational models can help further the field of electrocatalysis.[84]

■ ASSOCIATED CONTENT

Supporting Information

The Supporting Information is available free of charge at https://pubs.acs.org/doi/10.1021/acsenergylett.4c01897.

Experimental details regarding electrode/electrolyte prepration, electrochemical measurements, kinetic anal-

https://doi.org/10.1021/acsenergylett.4c01897
ACS Energy Lett. 2024, 9, 4724−4733

ysis, theoretical calculations, additional experimental Koutecký−Levich selectivity analysis, ORR rate data, benchmark comparisons, Tafel and ORR rate analysis, and DFT simulation results (PDF)

AUTHOR INFORMATION

Corresponding Author

Joaquin Resasco − *McKetta Department of Chemical Engineering, University of Texas at Austin, Austin, Texas 78712, United States;* orcid.org/0000-0001-6374-9877; Email: resasco@utexas.edu

Authors

Jay T. Bender − *McKetta Department of Chemical Engineering, University of Texas at Austin, Austin, Texas 78712, United States*

Rohan Yuri Sanspeur − *Department of Chemical Engineering, Carnegie Mellon University, Pittsburgh, Pennsylvania 15213, United States;* orcid.org/0000-0002-5583-8922

Angel E. Valles − *McKetta Department of Chemical Engineering, University of Texas at Austin, Austin, Texas 78712, United States*

Alyssa K. Uvodich − *McKetta Department of Chemical Engineering, University of Texas at Austin, Austin, Texas 78712, United States;* orcid.org/0009-0002-5539-8653

Delia J. Milliron − *McKetta Department of Chemical Engineering, University of Texas at Austin, Austin, Texas 78712, United States; Department of Chemistry, University of Texas at Austin, Austin, Texas 78712, United States;* orcid.org/0000-0002-8737-451X

John R. Kitchin − *Department of Chemical Engineering, Carnegie Mellon University, Pittsburgh, Pennsylvania 15213, United States;* orcid.org/0000-0003-2625-9232

Complete contact information is available at: https://pubs.acs.org/10.1021/acsenergylett.4c01897

Author Contributions

J.T.B. designed experiments, collected the data, and wrote the article. R.Y.S. performed all computational calculations. A.E.V. and A.K.U. assisted with collecting experimental data. J.R.K. guided the theoretical work. J.R. conceptualized and guided the work. All authors contributed to the discussion, review, and editing of the manuscript.

Notes

The authors declare no competing financial interest.

ACKNOWLEDGMENTS

We thank Dr. D. Davies for assistance with graphic design and S. M. J. Heffernan for assistance with designing preliminary experiments. J.T.B. gratefully acknowledges support of the National Science Foundation Graduate Research Fellowship Program (NSF GRFP) under Grant Nos. DGE-1610403 and DGE-2137420. A.K.U. gratefully acknowledges support from the National Science Foundation through the Center for Dynamics and Control of Materials: an NSF MRSEC under Cooperative Agreement No. DMR-2308817. J.R. and D.J.M. gratefully acknowledge support from the Welch Foundation under Grant Nos. F-2076 and F-1848, respectively. R.Y.S. and J.R.K. gratefully acknowledge support from the Army Research Office (ARO) project Award W911NF2010188.

REFERENCES

(1) Orella, M. J.; Román-Leshkov, Y.; Brushett, F. R. Emerging Opportunities for Electrochemical Processing to Enable Sustainable Chemical Manufacturing. *Curr. Opin. Chem. Eng.* **2018**, *20*, 159−167.

(2) Seh, Z. W.; Kibsgaard, J.; Dickens, C. F.; Chorkendorff, I.; Nørskov, J. K.; Jaramillo, T. F. Combining Theory and Experiment in Electrocatalysis: Insights into Materials Design. *Science* **2017**, *355*, No. eaad4998.

(3) Nørskov, J. K.; Bligaard, T.; Rossmeisl, J.; Christensen, C. H. Towards the Computational Design of Solid Catalysts. *Nat. Chem.* **2009**, *1*, 37−46.

(4) Colic, V.; Pohl, M. D.; Scieszka, D.; Bandarenka, A. S. Influence of the Electrolyte Composition on the Activity and Selectivity of Electrocatalytic Centers. *Catal. Today* **2016**, *262*, 24−35.

(5) Resasco, J.; Chen, L. D.; Clark, E.; Tsai, C.; Hahn, C.; Jaramillo, T. F.; Chan, K.; Bell, A. T. Promoter Effects of Alkali Metal Cations on the Electrochemical Reduction of Carbon Dioxide. *J. Am. Chem. Soc.* **2017**, *139*, 11277−11287.

(6) Bender, J. T.; Petersen, A. S.; Østergaard, F. C.; Wood, M. A.; Heffernan, S. M. J.; Milliron, D. J.; Rossmeisl, J.; Resasco, J. Understanding Cation Effects on the Hydrogen Evolution Reaction. *ACS Energy Lett.* **2023**, *8*, 657−665.

(7) Strmcnik, D.; Kodama, K.; van der Vliet, D.; Greeley, J.; Stamenkovic, V. R.; Marković, N. M. The Role of Non-Covalent Interactions in Electrocatalytic Fuel-Cell Reactions on Platinum. *Nat. Chem.* **2009**, *1*, 466−472.

(8) Görlin, M.; Halldin Stenlid, J.; Koroidov, S.; Wang, H.-Y.; Börner, M.; Shipilin, M.; Kalinko, A.; Murzin, V.; Safonova, O. V.; Nachtegaal, M.; et al. Key Activity Descriptors of Nickel-Iron Oxygen Evolution Electrocatalysts in the Presence of Alkali Metal Cations. *Nat. Commun.* **2020**, *11*, 6181.

(9) Zaffran, J.; Stevens, M. B.; Trang, C. D. M.; Nagli, M.; Shehadeh, M.; Boettcher, S. W.; Caspary Toroker, M. Influence of Electrolyte Cations on Ni(Fe)OOH Catalyzed Oxygen Evolution Reaction. *Chem. Mater.* **2017**, *29*, 4761−4767.

(10) Garcia, A. C.; Touzalin, T.; Nieuwland, C.; Perini, N.; Koper, M. T. M. Enhancement of Oxygen Evolution Activity of Nickel Oxyhydroxide by Electrolyte Alkali Cations. *Angew. Chem., Int. Ed.* **2019**, *58*, 12999−13003.

(11) Zhu, S.; Hu, X.; Zhang, L.; Shao, M. Impacts of Perchloric Acid, Nafion, and Alkali Metal Ions on Oxygen Reduction Reaction Kinetics in Acidic and Alkaline Solutions. *J. Phys. Chem. C* **2016**, *120*, 27452−27461.

(12) Strmcnik, D.; van der Vliet, D. F.; Chang, K.-C.; Komanicky, V.; Kodama, K.; You, H.; Stamenkovic, V. R.; Marković, N. M. Effects of Li^+, K^+, and Ba^{2+} Cations on the ORR at Model and High Surface Area Pt and Au Surfaces in Alkaline Solutions. *J. Phys. Chem. Lett.* **2011**, *2*, 2733−2736.

(13) Danilovic, N.; Subbaraman, R.; Strmcnik, D.; Paulikas, A. P.; Myers, D.; Stamenkovic, V. R.; Markovic, N. M. The Effect of Noncovalent Interactions on the HOR, ORR, and HER on Ru, Ir, and $Ru_{0.50}Ir_{0.50}$ Metal Surfaces in Alkaline Environments. *Electrocatalysis* **2012**, *3*, 221−229.

(14) Song, K.-T.; Zagalskaya, A.; Schott, C. M.; Schneider, P. M.; Garlyyev, B.; Alexandrov, V.; Bandarenka, A. S. Influence of Alkali Metal Cations on the Oxygen Reduction Activity of Pt_5Y and Pt_5Gd Alloys. *J. Phys. Chem. C* **2024**, *128*, 4969−4977.

(15) Kiguchi, F.; Nakamura, M.; Hoshi, N. Cation Effects on ORR Activity on Low-index Planes of Pd in Alkaline Solution. *Electrochemistry* **2021**, *89*, 145−147.

(16) Jiang, K.; Zhao, J.; Wang, H. Catalyst Design for Electrochemical Oxygen Reduction toward Hydrogen Peroxide. *Adv. Funct. Mater.* **2020**, *30*, 2003321.

(17) Kulkarni, A.; Siahrostami, S.; Patel, A.; Nørskov, J. K. Understanding Catalytic Activity Trends in the Oxygen Reduction Reaction. *Chem. Rev.* **2018**, *118*, 2302−2312.

(18) Marković, N. M.; Schmidt, T. J.; Stamenković, V.; Ross, P. N. Oxygen Reduction Reaction on Pt and Pt Bimetallic Surfaces: A Selective Review. *Fuel Cells* **2001**, *1*, 105−116.

(19) Stephens, I. E. L.; Bondarenko, A. S.; Grønbjerg, U.; Rossmeisl, J.; Chorkendorff, I. Understanding the Electrocatalysis of Oxygen Reduction on Platinum and Its Alloys. *Energy Environ. Sci.* **2012**, *5*, 6744−6762.
(20) Ringe, S.; Clark, E. L.; Resasco, J.; Walton, A.; Seger, B.; Bell, A. T.; Chan, K. Understanding Cation Effects in Electrochemical CO_2 Reduction. *Energy Environ. Sci.* **2019**, *12*, 3001−3014.
(21) Ringe, S. Cation Effects on Electrocatalytic Reduction Processes at the Example of the Hydrogen Evolution Reaction. *Curr. Opin. Electrochem.* **2023**, *39*, 101268.
(22) Hyung Kim, J.; Jang, H.; Bak, G.; Choi, W.; Yun, H.; Lee, E.; Kim, D.; Kim, J.; Young Lee, S.; Jeong Hwang, Y.; et al. The Insensitive Cation Effect on a Single Atom Ni Catalyst Allows Selective Electrochemical Conversion of Captured CO_2 in Universal Media. *Energy Environ. Sci.* **2022**, *15*, 4301−4312.
(23) Wei, C.; Rao, R. R.; Peng, J.; Huang, B.; Stephens, I. E. L.; Risch, M.; Xu, Z. J.; Shao-Horn, Y. Recommended Practices and Benchmark Activity for Hydrogen and Oxygen Electrocatalysis in Water Splitting and Fuel Cells. *Adv. Mater.* **2019**, *31*, 1806296.
(24) Kerschbaumer, A.; Wielend, D.; Leeb, E.; Schimanofsky, C.; Kleinbruckner, N.; Neugebauer, H.; Irimia-Vladu, M.; Serdar Sariciftci, N. How to Use a Rotating Ring-Disc Electrode (RRDE) Subtraction Method to Investigate the Electrocatalytic Oxygen Reduction Reaction? *Catal. Sci. Technol.* **2023**, *13*, 834−843.
(25) Suntivich, J.; Perry, E. E.; Gasteiger, H. A.; Shao-Horn, Y. The Influence of the Cation on the Oxygen Reduction and Evolution Activities of Oxide Surfaces in Alkaline Electrolyte. *Electrocatalysis* **2013**, *4*, 49−55.
(26) Lima, F. H. B.; Zhang, J.; Shao, M. H.; Sasaki, K.; Vukmirovic, M. B.; Ticianelli, E. A.; Adzic, R. R. Catalytic Activity-d-Band Center Correlation for the O_2 Reduction Reaction on Platinum in Alkaline Solutions. *J. Phys. Chem. C* **2007**, *111*, 404−410.
(27) Kumeda, T.; Tajiri, H.; Sakata, O.; Hoshi, N.; Nakamura, M. Effect of Hydrophobic Cations on the Oxygen Reduction Reaction on Single-crystal Platinum Electrodes. *Nat. Commun.* **2018**, *9*, 4378.
(28) Zamora Zeledón, J. A.; Stevens, M. B.; Gunasooriya, G. T. K. K.; Gallo, A.; Landers, A. T.; Kreider, M. E.; Hahn, C.; Nørskov, J. K.; Jaramillo, T. F. Tuning the Electronic Structure of Ag-Pd Alloys to Enhance Performance for Alkaline Oxygen Reduction. *Nat. Commun.* **2021**, *12*, 620.
(29) Singh, P.; Buttry, D. A. Comparison of Oxygen Reduction Reaction at Silver Nanoparticles and Polycrystalline Silver Electrodes in Alkaline Solution. *J. Phys. Chem. C* **2012**, *116*, 10656−10663.
(30) Damjanovic, A.; Genshaw, M. A.; Bockris, J. O. Hydrogen Peroxide Formation in Oxygen Reduction at Gold Electrodes: II. Alkaline Solution. *J. Electroanal. Chem. Interface Electrochem.* **1967**, *15*, 173−180.
(31) Schmidt, T. J.; Stamenkovic, V.; Arenz, M.; Markovic, N. M.; Ross, P. N. Oxygen Electrocatalysis in Alkaline Electrolyte: Pt(*hkl*), Au(*hkl*) and the Effect of Pd-modification. *Electrochim. Acta* **2002**, *47*, 3765−3776.
(32) Fischer, P.; Heitbaum, J. Mechanistic Aspects of Cathodic Oxygen Reduction. *J. Electroanal. Chem. Interface Electrochem.* **1980**, *112*, 231−238.
(33) Hansen, H. A.; Rossmeisl, J.; Nørskov, J. K. Surface Pourbaix Diagrams and Oxygen Reduction Activity of Pt, Ag and Ni(111) Surfaces Studied by DFT. *Phys. Chem. Chem. Phys.* **2008**, *10*, 3722−3730.
(34) Nørskov, J. K.; Rossmeisl, J.; Logadottir, A.; Lindqvist, L.; Kitchin, J. R.; Bligaard, T.; Jónsson, H. Origin of the Overpotential for Oxygen Reduction at a Fuel-Cell Cathode. *J. Phys. Chem. B* **2004**, *108*, 17886−17892.
(35) Holewinski, A.; Linic, S. Elementary Mechanisms in Electrocatalysis: Revisiting the ORR Tafel Slope. *J. Electrochem. Soc.* **2012**, *159*, H864.
(36) Chen, L. D.; Urushihara, M.; Chan, K.; Nørskov, J. K. Electric Field Effects in Electrochemical CO_2 Reduction. *ACS Catal.* **2016**, *6*, 7133−7139.
(37) Lang, N. D.; Holloway, S.; Nørskov, J. K. Electrostatic Adsorbate-Adsorbate Interactions: The Poisoning and Promotion of the Molecular Adsorption Reaction. *Surf. Sci.* **1985**, *150*, 24−38.
(38) Linic, S.; Barteau, M. A. On the Mechanism of Cs Promotion in Ethylene Epoxidation on Ag. *J. Am. Chem. Soc.* **2004**, *126*, 8086−8087.
(39) Montoya, J. H.; Shi, C.; Chan, K.; Nørskov, J. K. Theoretical Insights into a CO Dimerization Mechanism in CO_2 Electroreduction. *J. Phys. Chem. Lett.* **2015**, *6*, 2032−2037.
(40) Mortensen, J. J.; Hammer, B.; Nørskov, J. K. Alkali Promotion of N_2 Dissociation over Ru(0001). *Phys. Rev. Lett.* **1998**, *80*, 4333−4336.
(41) Sandberg, R. B.; Montoya, J. H.; Chan, K.; Nørskov, J. K. CO-CO Coupling on Cu Facets: Coverage, Strain and Field Effects. *Surf. Sci.* **2016**, *654*, 56−62.
(42) Kelly, S. R.; Kirk, C.; Chan, K.; Nørskov, J. K. Electric Field Effects in Oxygen Reduction Kinetics: Rationalizing pH Dependence at the Pt(111), Au(111), and Au(100) Electrodes. *J. Phys. Chem. C* **2020**, *124*, 14581−14591.
(43) Hübner, J. L.; Lucchetti, L. E. B.; Nong, H. N.; Sharapa, D. I.; Paul, B.; Kroschel, M.; Kang, J.; Teschner, D.; Behrens, S.; Studt, F.; et al. Cation Effects on the Acidic Oxygen Reduction Reaction at Carbon Surfaces. *ACS Energy Lett.* **2024**, *9*, 1331−1338.
(44) Lopes, P. P.; Strmcnik, D.; Jirkovsky, J. S.; Connell, J. G.; Stamenkovic, V.; Markovic, N. Double Layer Effects in Electrocatalysis: The Oxygen Reduction Reaction and Ethanol Oxidation Reaction on Au(111), Pt(111) and Ir(111) in Alkaline Media Containing Na and Li Cations. *Catal. Today* **2016**, *262*, 41−47.
(45) Monteiro, M. C. O.; Dattila, F.; Hagedoorn, B.; García-Muelas, R.; López, N.; Koper, M. T. M. Absence of CO_2 Electroreduction on Copper, Gold and Silver Electrodes without Metal Cations in Solution. *Nat. Catal.* **2021**, *4*, 654−662.
(46) Vos, R. E.; Koper, M. T. M. The Effect of Temperature on the Cation-Promoted Electrochemical CO_2 Reduction on Gold. *ChemElectroChem.* **2022**, *9*, No. e202200239.
(47) McGregor, J.-M.; Bender, J.; Petersen, A.; Canada, L.; Rossmeisl, J.; Brennecke, J.; Resasco, J. The Role of Organic Cations in the Electrochemical Reduction of CO_2 in Aprotic Solvents. *ChemRxiv*, 2024. DOI: 10.26434/chemrxiv−2024−wl1bg
(48) Zamora Zeledón, J. A.; Kamat, G. A.; Gunasooriya, G. T. K. K.; Nørskov, J. K.; Stevens, M. B.; Jaramillo, T. F. Probing the Effects of Acid Electrolyte Anions on Electrocatalyst Activity and Selectivity for the Oxygen Reduction Reaction. *ChemElectroChem.* **2021**, *8*, 2467−2478.
(49) Sundararaman, R.; Figueiredo, M. C.; Koper, M. T. M.; Schwarz, K. A. Electrochemical Capacitance of CO-Terminated Pt(111) Dominated by the CO−Solvent Gap. *J. Phys. Chem. Lett.* **2017**, *8*, 5344−5348.
(50) Sebastián-Pascual, P.; Shao-Horn, Y.; Escudero-Escribano, M. Toward Understanding the Role of the Electric Double Layer Structure and Electrolyte Effects on Well-Defined Interfaces for Electrocatalysis. *Curr. Opin. Electrochem.* **2022**, *32*, 100918.
(51) Trasatti, S.; Lust, E. In *Modern Aspects of Electrochemistry*; White, R. E., Bockris, J. O., Conway, B. E., Eds.; Springer US: 1999; pp 1−215.
(52) Le, J.; Iannuzzi, M.; Cuesta, A.; Cheng, J. Determining Potentials of Zero Charge of Metal Electrodes versus the Standard Hydrogen Electrode from Density-Functional-Theory-Based Molecular Dynamics. *Phys. Rev. Lett.* **2017**, *119*, 016801.
(53) Frumkin, A. N.; Petrii, O. A. Potentials of Zero Total and Zero Free Charge of Platinum Group Metals. *Electrochim. Acta* **1975**, *20*, 347−359.
(54) Petrii, O. A. Zero Charge Potentials of Platinum Metals and Electron Work Functions (Review). *Russ. J. Electrochem.* **2013**, *49*, 401−422.
(55) Martínez-Hincapié, R.; Climent, V.; Feliu, J. M. New Probes to Surface Free Charge at Electrochemical Interfaces with Platinum Electrodes. *Current Opinion in Electrochemistry* **2019**, *14*, 16−22.

(56) Climent, V.; Gómez, R.; Feliu, J. M. Effect of Increasing Amount of Steps on the Potential of Zero Total Charge of Pt(111) Electrodes. *Electrochim. Acta* **1999**, *45*, 629−637.
(57) Cuesta, A. Measurement of the Surface Charge Density of CO-saturated Pt(111) Electrodes as a Function of Potential: The Potential of Zero Charge of Pt(111). *Surf. Sci.* **2004**, *572*, 11−22.
(58) Sanspeur, R. Y.; Heras-Domingo, J.; Kitchin, J. R.; Ulissi, Z. WhereWulff: A Semiautonomous Workflow for Systematic Catalyst Surface Reactivity under Reaction Conditions. *J. Chem. Inf. Model.* **2023**, *63*, 2427−2437.
(59) Taylor, C. D.; Wasileski, S. A.; Filhol, J.-S.; Neurock, M. First Principles Reaction Modeling of the Electrochemical Interface: Consideration and Calculation of a Tunable Surface Potential from Atomic and Electronic Structure. *Phys. Rev. B* **2006**, *73*, 165402.
(60) Filhol, J.-S.; Neurock, M. Elucidation of the Electrochemical Activation of Water over Pd by First Principles. *Angew. Chem., Int. Ed.* **2006**, *45*, 402−406.
(61) Duan, Z.; Henkelman, G. Theoretical Resolution of the Exceptional Oxygen Reduction Activity of Au(100) in Alkaline Media. *ACS Catal.* **2019**, *9*, 5567−5573.
(62) Derry, G. N.; Kern, M. E.; Worth, E. H. Recommended Values of Clean Metal Surface Work Functions. *J. Vac. Sci. Technol. A* **2015**, *33*, 060801.
(63) Trasatti, S. Work Function, Electronegativity, and Electrochemical Behaviour of Metals: II. Potentials of Zero Charge and "Electrochemical" Work Functions. *Journal of Electroanalytical Chemistry and Interfacial Electrochemistry* **1971**, *33*, 351−378.
(64) Kelly, S. R.; Heenen, H. H.; Govindarajan, N.; Chan, K.; Nørskov, J. K. OH Binding Energy as a Universal Descriptor of the Potential of Zero Charge on Transition Metal Surfaces. *J. Phys. Chem. C* **2022**, *126*, 5521−5528.
(65) Ringe, S.; Hörmann, N. G.; Oberhofer, H.; Reuter, K. Implicit Solvation Methods for Catalysis at Electrified Interfaces. *Chem. Rev.* **2022**, *122*, 10777−10820.
(66) Levell, Z.; Le, J.; Yu, S.; Wang, R.; Ethirajan, S.; Rana, R.; Kulkarni, A.; Resasco, J.; Lu, D.; Cheng, J.; et al. Emerging Atomistic Modeling Methods for Heterogeneous Electrocatalysis. *Chem. Rev.* **2024**, *124*, 8620−8656.
(67) Li, X.-Y.; Chen, A.; Yang, X.-H.; Zhu, J.-X.; Le, J.-B.; Cheng, J. Linear Correlation between Water Adsorption Energies and Volta Potential Differences for Metal/Water Interfaces. *J. Phys. Chem. Lett.* **2021**, *12*, 7299−7304.
(68) Mathew, K.; Kolluru, V. S. C.; Mula, S.; Steinmann, S. N.; Hennig, R. G. Implicit Self-Consistent Electrolyte Model in Plane-Wave Density-Functional Theory. *J. Chem. Phys.* **2019**, *151*, 234101.
(69) Hinsch, J. J.; Bouzid, A.; Barker, J. C.; White, J. J.; Mortier, F.; Zhao, H.; Wang, Y. Revisiting the Electrified Pt(111)/Water Interfaces through an Affordable Double-Reference Ab Initio Approach. *J. Phys. Chem. C* **2023**, *127*, 19857−19866.
(70) Bramley, G.; Nguyen, M.-T.; Glezakou, V.-A.; Rousseau, R.; Skylaris, C.-K. Reconciling Work Functions and Adsorption Enthalpies for Implicit Solvent Models: A Pt (111)/Water Interface Case Study. *J. Chem. Theory Comput.* **2020**, *16*, 2703−2715.
(71) Sakong, S.; Forster-Tonigold, K.; Groß, A. The Structure of Water at a Pt(111) Electrode and the Potential of Zero Charge Studied from First Principles. *J. Chem. Phys.* **2016**, *144*, 194701.
(72) Sakong, S.; Groß, A. The Electric Double Layer at Metal-Water Interfaces Revisited Based on a Charge Polarization Scheme. *J. Chem. Phys.* **2018**, *149*, 084705.
(73) Wang, Y.; Gordon, E.; Ren, H. Mapping the Potential of Zero Charge and Electrocatalytic Activity of Metal−Electrolyte Interface via a Grain-by-Grain Approach. *Anal. Chem.* **2020**, *92*, 2859−2865.
(74) Xu, P.; von Rueden, A. D.; Schimmenti, R.; Mavrikakis, M.; Suntivich, J. Optical Method for Quantifying the Potential of Zero Charge at the Platinum−Water Electrochemical Interface. *Nat. Mater.* **2023**, *22*, 503−510.
(75) Domke, K.; Herrero, E.; Rodes, A.; Feliu, J. M. Determination of the potentials of zero total charge of Pt (100) stepped surfaces in the [011] zone. Effect of the step density and anion adsorption. *J. Electroanal. Chem.* **2003**, *552*, 115−128.
(76) Chen, Q.-S.; Solla-Gullón, J.; Sun, S.-G.; Feliu, J. M. The potential of zero total charge of Pt nanoparticles and polycrystalline electrodes with different surface structure: The role of anion adsorption in fundamental electrocatalysis. *Electrochim. Acta* **2010**, *55*, 7982−7994.
(77) Ibach, H. Vibration Spectroscopy of Water on Stepped Gold Surfaces. *Surf. Sci.* **2010**, *604*, 377−385.
(78) Wang, Y.-H.; Zheng, S.; Yang, W.-M.; Zhou, R.-Y.; He, Q.-F.; Radjenovic, P.; Dong, J.-C.; Li, S.; Zheng, J.; Yang, Z.-L.; et al. In Situ Raman Spectroscopy Reveals the Structure and Dissociation of Interfacial Water. *Nature* **2021**, *600*, 81−85.
(79) Delley, M. F.; Nichols, E. M.; Mayer, J. M. Electrolyte Cation Effects on Interfacial Acidity and Electric Fields. *J. Phys. Chem. C* **2022**, *126*, 8477−8488.
(80) Kumeda, T.; Kondo, K.; Tanaka, S.; Sakata, O.; Hoshi, N.; Nakamura, M. Surface Extraction Process During Initial Oxidation of Pt(111): Effect of Hydrophilic/Hydrophobic Cations in Alkaline Media. *J. Am. Chem. Soc.* **2024**, *146*, 10312−10320.
(81) Jung, O.; Jackson, M. N.; Bisbey, R. P.; Kogan, N. E.; Surendranath, Y. Innocent Buffers Reveal the Intrinsic pH- and Coverage-Dependent Kinetics of the Hydrogen Evolution Reaction on Noble Metals. *Joule* **2022**, *6*, 476−493.
(82) Chang, X.; Vijay, S.; Zhao, Y.; Oliveira, N. J.; Chan, K.; Xu, B. Understanding the Complementarities of Surface-Enhanced Infrared and Raman Spectroscopies in CO Adsorption and Electrochemical Reduction. *Nat. Commun.* **2022**, *13*, 2656.
(83) Zhao, K.; Xiong, H.; Xiao, Y.; Su, H.; Wu, D.; Chang, X.; Lu, Q.; Xu, B. Understanding the Effect of Specific Adsorption on the Vibrational Stark Effect of Adsorbates on an Electrode Surface via Surface Enhanced Spectroscopy. *Inorg. Chem. Front.* **2024**, *11*, 756−768.
(84) Resasco, J.; Abild-Pedersen, F.; Hahn, C.; Bao, Z.; Koper, M. T. M.; Jaramillo, T. F. Enhancing the Connection between Computation and Experiments in Electrocatalysis. *Nat. Catal.* **2022**, *5*, 374−381.

https://doi.org/10.1021/acsenergylett.4c01897
ACS Energy Lett. 2024, 9, 4724−4733